ENERGY INTERACTION BETWEEN THE TROPOSPHERE AND STRATOSPHERE

by
LAWRENCE S. HANSROTE
B.S., Virginia Polytechnic Institute
(1952)

JOSEPH K. LAMBERT
B.S., Loras College
(1951)

SUBMITTED IN PARTIAL FULFILLMENT OF THE
REQUIREMENTS FOR THE DEGREE OF
MASTER OF SCIENCE
at the
MASSACHUSETTS INSTITUTE OF TECHNOLOGY
(1960)

Signature of Authors . . . .

. . . .
Department of Meteorology, 21 May 1960

Certified by . . . .
Thesis Supervisor

Accepted by. . . . .
Chairman, Departmental Committee on Graduate Students

ENERGY INTERACTION BETWEEN THE TROPOSPHERE AND STRATOSPHERE

by

Lawrence S. Hansrote
Joseph K. Lambert

Submitted to the Department of Meteorology on May 21, 1960,
in Partial Fulfillment of the Requirements for the
Degree of Master of Science

ABSTRACT

We have obtained a value for the time eddy term and the mean eddy term of the advection of kinetic energy and of the $\phi\omega$ component of the source term of the kinetic energy equation for the Northern Hemisphere above 20° north and 150 mb. These were compared with the time eddy term value of the $\omega\alpha$ component of the source term in the kinetic energy equation.

Thesis Supervisor: Victor P. Starr
Title: Professor of Meteorology

ACKNOWLEDGEMENTS

First, and foremost, the authors wish to express their sincere appreciation to Professor Victor P. Starr for his suggestion of the problem investigated by this thesis, and for his guidance throughout.

Acknowledgement is also made to Major Clayton E. Jensen for it was through him that the raw data, on which all our computations are based, was obtained. The authors are also indebted to Maj. Jensen for his valuable discussions and comments throughout the thesis.

Aid in long and tedious computations was given by Mrs. Janet Dwyer and her staff at the Geophysics Research Directorate, L. G. Hanscom Field. Thanks also to Miss Isabel Kole for aid in preparing the charts.

TABLE OF CONTENTS

I. INTRODUCTION

A. The General Problem

In recent years quite a few studies have been made on the troposphere with regard to energy considerations and the general circulation. The most recent of these studies have been conducted by Saltzman and Fleisher (1) and White and Saltzman (2). Very little research, however, has been done in regard to energy considerations of the stratosphere. This is not too surprising since observational data, on a hemispheric scale, has been quite sparse at these higher levels. However, following the International Geophysical Year, more data than ever before at high levels (300 mb and above) was made available for research and analysis.

There has been one instance where research was done on the lower stratosphere with regard to energy considerations. Here the reference is to the paper of White and Nolan (3) on the potential to kinetic energy process in the stratosphere. They found, for the very limited period and region under study, that the production of horizontal kinetic energy in the lower levels of the stratosphere (100 mb and 50 mb) was negative, being nearly zero at 100 mb, as was suggested by Starr (4). This would seem to make sense physically since the stratosphere is generally considered to be extremely stable hydrostatically. This stability would of course resist natural convective activity, and hence, one would suspect the conversion of potential to kinetic energy to be zero or negative.

Another bit of evidence supporting the theory that this conversion in the stratosphere should be in the kinetic to potential energy sense, resulting in an averaged "forced motion" at these levels (4), is the study conducted by White (5) which noted a counter-gradient flow of heat at these levels.

Thus, if we accept the hypothesis that the stratosphere is a kinetic energy sink, the kinetic energy must be replenished through some means or eventually the stratospheric winds would run down like a gigantic clock which someone forgot to wind. Discounting the possibility that kinetic energy sources might occur in the higher levels of the stratosphere, which seems unlikely, and be brought downward to reinforce the stratospheric winds leaves only the following alternative solutions; namely, that the stratosphere motions are maintained by the advection of the necessary energy upward from the troposphere (4), or there is another source of energy to draw upon.

It is this replenishing of the kinetic energy which the authors set out to evaluate for a month (April 1958) over the Northern

Hemisphere from 20 degrees north to 80 degrees north and at 150 mb.

When we speak of data at 150 mb, we are speaking in all instances of data averaged properly between 200 mb and 100 mb.

It is true that the level of 150 mb will not be in all instances in the stratosphere, but over much of the hemisphere 150 mb might be expected to be in the lower stratosphere. The level of 150 mb was chosen not by chance, but as that at which the authors could obtain vertical velocity data and still have a sufficient coverage, for hemispheric computation.

B. The Thesis Problem

The thesis problem is an investigation into the evaluation of the modes of replenishing the kinetic energy of the stratosphere that is lost due to an apparent conversion into potential energy. The thesis' aims are:

(1) To determine the amount of kinetic energy advected into the atmosphere above 150 mb over a portion of the Northern Hemisphere between 20 degrees north and 80 degrees north.

(2) To determine the contribution to the kinetic energy of the stratosphere by vertical advection of potential energy from the troposphere.

(3) To integrate the results of aims (1) and (2) with results

obtained from others (6) for the conversion term in the time rate of change of kinetic energy equation.

II. APPROACH TO PROBLEM

A. Mathematical and Physical Considerations

Starting with a coordinate system in which pressure is the vertical coordinate and the use of the hydrostatic equation, we can write the equation of motion for the horizontal wind as

$$\frac{d\vec{c}}{dt} + f\vec{k}\times\vec{c} = -\nabla\phi - \vec{F} \qquad (1)$$

where $\vec{C}$ is the horizontal vector wind, f is the Coriolis parameter, $\vec{k}$ is the unit vector in the vertical, ∇ is the two-dimensional del operator of a pressure surface, $\phi = gz$ is the geopotential of an isobaric surface, and $\vec{F}$ is the vector frictional force per unit mass. Next, if we take the scalar product of $\vec{C}$ with (1) and expand the total derivative into the local time rate of change plus the advective terms, we obtain the energy equation for the horizontal motions in the following form

$$\frac{\partial k}{\partial t} + \vec{c}\cdot\nabla k + \omega\frac{\partial k}{\partial p} = -\vec{c}\cdot\nabla\phi - D \qquad (2)$$

where now $k = \frac{c^2}{2}$ is the kinetic energy of horizontal motion per unit mass, $D = \vec{c}\cdot\vec{F}$ is the rate of frictional dissipation of kinetic energy per unit mass and $\omega = \frac{dp}{dt}$. If we integrate (2) over mass we have

$$\int_M \frac{\partial k}{\partial t} dm + \int_M \vec{c}\cdot\nabla k\, dm + \int_M \omega \frac{\partial k}{\partial p} dm = -\int_M \vec{c}\cdot\nabla\Phi\, dm - \int_M D\, dm \tag{3}$$

If we inspect (3) we have on the left-hand side the <u>total</u> time rate of change of kinetic energy integrated over mass and thus we can look upon the right-hand side now as a source term (S) and a dissipative term (D^*). We then have

$$S = -\int_M \vec{c}\cdot\nabla\Phi\, dm \quad ; \quad D^* = \int_M D\, dm \tag{4}$$

S can be written as

$$S = -\int_M \nabla\cdot\vec{c}\,\Phi\, dm + \int_M \Phi\,\nabla\cdot\vec{c}\, dm \tag{5}$$

Using the equation of continuity

$$\frac{\partial\omega}{\partial p} = -\nabla\cdot\vec{c} \tag{6}$$

(5) becomes

$$S = -\int_M \nabla\cdot\vec{c}\,\Phi\, dm - \int_M \Phi \frac{\partial\omega}{\partial p} dm \tag{7}$$

The assumption is now introduced that for the hemisphere the divergence term is negligible. Rewriting the S term and using the hydrostatic equation

$$\frac{\partial\Phi}{\partial p} = -\frac{1}{\rho} = -\alpha \tag{8}$$

where ρ is density and α is specific volume. We have

$$S = -\int_M \frac{\partial \phi \omega}{\partial p} dm - \int_M \omega \alpha \, dm \tag{9}$$

Returning now to the left-hand side of (3) and rewriting we have

$$\int_M \frac{\partial k}{\partial t} dm + \int_M \nabla \cdot \vec{c} \, k \, dm - \int_M k \nabla \cdot \vec{c} \, dm + \int_M \omega \frac{\partial k}{\partial p} dm = S - D^* \tag{10}$$

Using (6), (10) becomes

$$\int_M \frac{\partial k}{\partial t} dm + \int_M \nabla \cdot \vec{c} \, k \, dm + \int_M k \frac{\partial \omega}{\partial p} dm + \int_M \omega \frac{\partial k}{\partial p} dm = S - D^* \tag{11}$$

We again introduce the assumption that the divergence term is negligible and (11) becomes

$$\int_M \frac{\partial k}{\partial t} dm + \int_M \frac{\partial k}{\partial p} \omega \, dm = -\int_M \frac{\partial \phi \omega}{\partial p} dm - \int_M \omega \alpha \, dm - \int_M D \, dm \tag{12}$$

Since we are concerned in this thesis with that portion of the atmosphere enclosed by the 20-degree north latitude circle and the 80-degree north latitude circle and above the 150-mb level, we will integrate (12) over the mass of this part of the atmosphere. Note that the limits of integration are taken from low pressure to high pressure.

$$\frac{\partial}{\partial t} \int_M k \, dm + \frac{1}{g} \iiint_{p=0}^{p=150\text{mb}} \frac{\partial (k\omega)}{\partial p} dx\,dy\,dp = -\frac{1}{g} \iiint_{p=0}^{p=150\text{mb}} \frac{\partial \phi \omega}{\partial p} dx\,dy\,dp - \frac{1}{g} \iiint_{p=0}^{p=150\text{mb.}} \omega \alpha \, dx\,dy\,dp - \int_M D \, dm \tag{13}$$

Integrating over pressure the second and third terms in (13) give

$$\frac{1}{g}\iint\left[k\omega)_{150}-k\omega)_{0}\right]dx\,dy=\frac{1}{g}\iint k\omega)_{150}\,dx\,dy \quad \text{SINCE } \omega_0=0 \qquad (14)$$

$$-\frac{1}{g}\iint\left[\phi\omega)_{150}-\phi\omega)_{0}\right]dx\,dy=-\frac{1}{g}\iint \phi\omega)_{150}\,dx\,dy \quad \text{SINCE } \omega_0=0 \qquad (15)$$

Using the approximate relation $\omega \approx -\rho g w$ we can now write (13) as

$$\frac{d}{dt}\int_M k\,dm=\rho\iint kw)_{150}\,dx\,dy+\rho\iint \phi w)_{150}\,dx\,dy-\frac{1}{g}\iiint_{p=0}^{p=150\,mb}\omega\alpha\,dx\,dy\,dp-\int_M D\,dm \qquad (16)$$

In evaluating the terms in equation (16) we are led to the conclusion that the time rate of change of the total horizontal kinetic energy within a fixed mass is the consequence of the following terms of the right-hand side:

1. The advection term which gives the rate at which the kinetic energy is being transported across the 150-mb level. This can be considered a redistribution term, and is represented by

$$A=\iint k\rho w\,dx\,dy$$

This term will disappear if the entire mass of the atmosphere is considered.

2. The source term of which there are two components arising from our selection of coordinates, as compared to the term Starr (4) calls S . We also choose to call these two components an S term.

$$S=\iint \phi\rho w\,dx\,dy-\frac{1}{g}\iiint \omega\alpha\,dx\,dy\,dp$$

3. The frictional term which ordinarily is a dissipative process and is represented by

$$D^* = \int_M D\,dm$$

Rewriting (16) in symbolic form gives

$$\frac{\partial}{\partial t}\int k\,dm = A + S - D^* \qquad (17)$$

We will consider that the change of kinetic energy over the period of the month is essentially zero; this would be true in a long-term mean. We will then write (17) in the following form.

$$A + S = D^* \qquad (18)$$

This states that if the kinetic energy, above 150 mb in our case, is to remain constant, the dissipation must be balanced by the advection of kinetic energy across the pressure surface or by what we have chosen to call the source term.

Let us examine these terms in order, the first being A. Since there is essentially no advection of kinetic energy through the upper boundary; i.e., at $p=0$, this leaves only the 150-mb surface as the lower boundary. Now since the stratosphere is not gaining or losing mass over the long-term mean we may write

$$\iint \rho \bar{w}\,dx\,dy = 0 \qquad (19)$$

and in order for A to be non-zero, we must have a correlation between k and ρw. Further if there are to be large values for the advection term then large values of k must be associated with areas where positive values of ρw occur.

Next if we take a look at the S term we see this is the sum of a conversion term and of an advection term. As was mentioned before this is called a source term because of its origin in the mathematical development. It is noted in (2) that the total time rate of change of kinetic energy changes by a dissipative term and a scalar product. It is from this equation that the source term evolves.

In order for $\iint \phi \rho w \, dx\, dy$ to be non-zero, there must be a correlation between ϕ and ρw; further if there is to be a large positive value for this term, then large values of ϕ must be associated where positive values of ρw occur. The $-\frac{1}{g}\iiint \omega \alpha \, dx\, dy\, dp$ term of S was shown by White and Saltzman (2) to require a spacewise correlation between ω and α over the area of an isobaric surface. It is with this term that we compared our calculated values of A and $\iint \rho w \phi \, dx\, dy$.

Finally in our mathematical manipulation, the frictional term, D^* is simply the work done by the fluid against frictional stresses arising from the viscosity of the fluid.

B. Computational Procedures

1. Computation of Vertical Velocities. The greatest difficulty in evaluating the advection term $\iint k\rho\omega\,dx\,dy$ and the $\iint \Phi\rho\omega\,dx\,dy$ term from the sounding data is that of determining the field of vertical motion, ω. The formula used for ω is the following,

$$\omega \approx -\frac{\frac{\partial T}{\partial t} + \vec{c}\cdot\nabla_p T}{\gamma_D - \gamma} \tag{20}$$

This equation is derived using the assumption that the change in potential temperature for the 200-mb to 100-mb level is zero. This would seem to be a reasonable assumption in this layer of no condensation. The finite difference form of (20) as used in the computations of ω may be found in Appendix 2.

2. Density Values. The value of ρ used in all calculations pertaining to the $\iint k\rho\omega\,dx\,dy$ term and the $\iint \Phi\rho\omega\,dx\,dy$ term were obtained by averaging the standard NACA values of at 200 and 100 mb and at a temperature of 218°A. The value used for 150 mb was 2.4×10^{-4} g cm^{-3}.

3. Computation of the Kinetic Energy Term k. The horizontal kinetic energy per unit mass for 150 mb was computed for each 12-hour period using the wind speeds at the 200- and 100-mb levels for two successive 12-hour radiosonde observations.

4. Statistical Analysis of the Advection Term. In order to

evaluate the advection term across the 150-mb surface over that portion of the atmosphere we have chosen in both space and time, a statistical analysis was incorporated. The derivation of this method in detail is found in Appendix 3. The resulting expression for the advection term is

$$\left\{\left[\overline{k\rho\omega}\right]\right\} = \left\{\left[\bar{k}\right]\left[\rho\bar{\omega}\right]\right\} + \left\{\left[\bar{k}'\rho\bar{\omega}'\right]\right\} + \left\{\left[\overline{k'\rho\omega'}\right]\right\} \tag{21}$$

The first term on the right-hand side is difficult to evaluate as the reliability of $\left[\rho\bar{\omega}\right]$ is dubious, whereas the remaining two terms are deviation terms and can be measured more easily. No effort will be made to evaluate the first term. The last two terms referred to as the "mean eddy term" and the "time eddy term", respectively, were evaluated using expansions of the terms as shown in Appendix 3. Thus, we will rewrite (21) in the form

$$\left\{\left[\overline{k\rho\omega}\right]\right\} - \left\{\left[\bar{k}\right]\left[\rho\bar{\omega}\right]\right\} = \left\{\left[\bar{k}'\rho\bar{\omega}'\right]\right\} + \left\{\left[\overline{k'\rho\omega'}\right]\right\} \tag{22}$$

The correlation coefficient, r, between k and $\rho\omega$ for each station was calculated as follows

$$r(k,\rho\omega) = \frac{\overline{k'\omega'}}{\left(\sqrt{\overline{k^2} - \bar{k}^2}\right)\left(\sqrt{\overline{\omega^2} - \bar{\omega}^2}\right)} \tag{23}$$

See Appendix 3 for further breakdown on this formula.

5. Statistical Treatment of the $\iint \phi\rho\omega \, dx dy$ term. This term

was treated statistically in an analogous fashion to the advection term. Only the right-hand side of the following equation was evaluated

$$\{[\overline{\Phi\rho\omega}]\}-\{[\bar{\Phi}][\rho\bar{\omega}]\}=\{[\bar{\Phi}'\rho\bar{\omega}']\}+\{[\overline{\Phi'\rho\omega'}]\} \qquad (24)$$

The correlation coefficient, r, between Φ and $\rho\omega$ for each station was calculated as follows

$$r(\phi,\rho\omega)=\frac{\overline{\phi'\omega'}}{\left(\sqrt{\overline{\Phi^2}-\bar{\Phi}^2}\right)\left(\sqrt{\overline{\omega^2}-\bar{\omega}^2}\right)} \qquad (25)$$

See Appendix 3 for further breakdown on this formula.

6. Determination of $\overline{\omega'\alpha'}$ from $\overline{\omega'T'}$ data. As only values of $\overline{\omega'T'}$ were made available to the authors for the layers of 200 to 100 mb and from 100 to 50 mb it was necessary to convert these values to the same expression we encounter in the source term, i.e., $\overline{\omega'\alpha'}$. The relation used was

$$\overline{\omega'\alpha'}=\frac{R}{p}\rho g\,\overline{\omega'T'} \qquad (26)$$

where ρ is now a mean value of the density for the 150- to 100-mb level and for the 100- to 50-mb level. The values used were

2.0×10^{-4} gm cm^{-3}

1.1×10^{-4} gm cm^{-3}

The values used for p were 125 and 75 mb.

It was then necessary to multiply the value of $\{[\overline{\omega'\alpha'}]\}$ obtained for each layer by 51 grams, which is the mass of the atmosphere in each of the two layers above each cm^2; this then gives the values in ergs cm^{-2} sec^{-1}.

C. Available Data

Data from 70 selected WBAN stations and 17 Russian stations in the form of mean values for ω (cm sec^{-1}) for the 12-hour interval between radiosonde runs, the height values (meters) for each radiosonde run, and the values of the wind direction and speed (meters sec^{-1}) for the 200- to 100-mb level for each available observation for the month of April 1958 were made available to the authors by Major Clayton E. Jensen, from data received from the Air Weather Service Climatic Center at Asheville, North Carolina. In addition, for the purpose of obtaining a more complete study of the energy mechanisms, values of $\overline{\omega' T'}$ for the 200- to 100-mb level and the 100- to 50-mb level were made available by Major Jensen. Necessary values needed for our computations were also computed by the authors for Aden, Khartoum and Saigon.

In areas of dense data, i.e., the United States, stations with a number of observations below 10 were discarded, but over areas of sparse data this was not done. Monthly mean data for each station may be found in Appendix 4.

III. RESULTS

Part of the results of the work done by the authors is presented in Tables 2 through 13. The values of $\overline{\phi'\rho\omega}$ and of the correlation coefficient $r(\phi, \rho\omega)$ were obtained by using an IBM 650 computer.

All averages around the latitude circles were multiplied by the cosine of the latitude as the proper weighting factor. For obtaining the average over time and the portion of the atmosphere considered, the values for the latitude circles were summed and divided by the sum of the cosines of the latitudes as the proper weighting factor.

Table 1. Values are in ergs cm^{-2} sec^{-1}

$$\left\{[\overline{k\rho\omega}]\right\} - \left\{[\bar{k}][\rho\bar{\omega}]\right\} = 11.5$$

$$\left\{[\overline{\Phi\rho\omega}]\right\} - \left\{[\bar{\Phi}][\rho\bar{\omega}]\right\} = 73.2$$

$$-\left\{[\overline{\omega'\alpha'}]\right\} = -36.2$$

Table 2. Values of $\overline{w}$ (cm sec^{-1}) determined from Chart 1 for each grid point.

	20°	30°	40°	50°	60°	70°	80°
80°E	x	x	-0.1	0.16	0.04	0.06	0.02
70	x	x	x	0.17	-0.10	0.06	0.02
60	x	x	-0.03	0.07	-0.20	0.06	0.02
50	x	0.00	-0.01	0.13	-0.12	0.06	0.02
40	0.2	0.30	0.06	0.08	0.04	0.06	0.02
30	-1.2	-0.20	0.12	0.15	0.03	0.06	0.02
20	-0.15	-0.20	0.01	0.04	0.03	0.06	0.02
10	x	-0.08	-0.15	-0.01	0.04	0.06	0.02
0	x	-0.04	-0.12	-0.05	0.10	0.10	0.02
10°W	x	-0.05	-0.12	-0.05	0.18	0.22	0.02
20	-0.05	-0.10	-0.25	0.02	0.27	0.27	0.02
30	-0.13	-0.28	-0.21	0.17	0.40	0.33	0.02
40	-0.18	-0.28	-0.15	0.20	0.43	0.34	0.02
50	-0.17	-0.29	-0.21	-0.06	0.38	0.29	0.02
60	-0.19	-0.32	-0.25	-0.04	0.25	0.24	0.02
70	-0.24	-0.25	-0.20	-0.08	0.10	0.16	0.02
80	-0.20	-0.05	-0.00	-0.26	0.02	0.06	0.02
90	-0.05	-0.20	-0.10	-0.17	-0.01	0.05	0.02
100	0.05	0.10	-0.10	0.00	-0.01	0.05	0.02
110	0.05	0.11	-0.30	0.05	0.02	0.03	0.02
120	0.05	-0.02	-0.30	0.02	0.02	0.03	0.02
130	-0.10	-0.29	-0.15	-0.02	0.00	0.02	0.02
140	-0.10	-0.33	-0.18	-0.10	-0.02	0.02	0.02
150	0.06	-0.13	-0.16	-0.12	-0.03	0.02	0.02
160	-0.05	-0.12	-0.11	-0.07	-0.05	0.02	0.02
170	-0.30	-0.30	-0.20	-0.01	-0.01	0.05	0.02
180	-0.25	-0.23	-0.17	-0.05	0.12	0.05	0.02
170°E	-0.09	-0.05	0.04	-0.05	0.10	0.05	0.02
160	-0.08	-0.02	0.07	0.13	0.06	0.03	0.02
150	-0.10	-0.05	0.07	0.16	0.05	0.02	0.02
140	-0.05	0.05	0.09	0.14	-0.02	0.02	0.02
130	0.05	0.12	0.00	-0.10	-0.02	0.03	0.02
120	0.05	0.05	-0.07	-0.14	0.10	0.05	0.02
110	0.01	0.00	x	0.22	0.22	0.07	0.02
100	x	x	x	0.18	0.18	0.08	0.02
90	x	x	x	0.17	0.12	0.07	0.02

Table 3. Values of $\bar{Z}$ (meters) determined from Chart 2 for each grid point.

	20°	30°	40°	50°	60°	70°	80°
80°E	x	x	13900	13760	13650	13510	13440
70	x	x	x	13840	13680	13560	13440
60	x	x	14140	13910	13730	13590	13440
50	x	14330	14120	13950	13770	13610	13440
40	14460	14210	14050	13920	13780	13630	13440
30	14410	14170	13980	13850	13780	13620	13440
20	14430	14220	14030	13850	13750	13600	13400
10	x	14240	14030	13850	13930	13580	13440
0	x	14210	13900	13820	13680	13550	13440
10°W	x	14160	13950	13800	13670	13520	13440
20	14320	14170	14000	13810	13670	13510	13440
30	14340	14240	14090	13870	13700	13520	13440
40	14400	14290	14100	13880	13730	13550	13440
50	14460	14300	14080	13870	13740	13560	13440
60	14460	14270	14030	13840	13730	13560	13440
70	14460	14260	14000	13840	13720	13550	13440
80	14450	14270	14000	13830	13690	13540	13440
90	14430	14250	14000	13820	13670	13530	13440
100	14440	14240	13950	13780	13660	13500	13440
110	14450	14260	13940	13780	13650	13500	13400
120	14450	14260	13960	13800	13660	13510	13440
130	14450	14270	14000	13830	13670	13520	13440
140	14470	14310	14020	13830	13680	13530	13440
150	14500	14310	14030	13820	13690	13550	13440
160	14500	14250	13950	13770	13660	13560	13440
170	14450	14190	13860	13680	13630	13500	13440
180	14440	14210	13840	13640	13510	13460	13440
170°E	14500	14320	13940	13660	13490	13430	13440
160	14540	14420	14100	13690	13540	13430	13440
150	14540	14420	14100	13700	13580	13440	13440
140	14530	14320	14020	13720	13610	13460	13440
130	14520	14260	14000	13760	13630	13470	13440
120	14520	14280	14060	13800	13620	13470	13440
110	14510	14260	x	13810	13600	13450	13440
100	x	x	x	13770	13580	13430	13440
90	x	x	x	13740	13580	13450	13440

Table 4. Values of C_n (meters^{2}sec^{-2}) determined from Chart 3 for each grid point.

	20°	30°	40°	50°	60°	70°	80°
80°E	x	x	2200	2300	1200	400	200
70	x	x	x	1500	600	300	200
60	x	x	1300	1100	500	300	200
50	x	2500	1300	1100	500	400	200
40	2500	1600	1400	1000	500	700	200
30	3000	3000	2000	1000	1000	700	200
20	5000	5800	3800	2000	1100	600	200
10	x	6700	3500	1000	800	400	200
0	x	5000	2000	750	400	200	200
10°W	x	3800	1200	1100	400	100	200
20	3500	3000	2100	1200	500	100	200
30	3200	2700	2100	1500	600	300	200
40	2500	2400	2100	1500	500	400	200
50	2000	2400	2200	1800	500	600	200
60	1800	3000	2200	2100	1000	700	200
70	2000	4500	2500	1200	800	600	200
80	1800	5500	2500	800	400	400	200
90	2500	7500	1400	1400	500	300	200
100	4000	6800	2500	750	700	300	200
110	4000	5100	2000	500	500	300	200
120	3000	3600	1500	1000	400	200	200
130	2800	3300	1400	600	300	100	200
140	2000	2700	1500	700	400	100	200
150	1400	1800	1500	800	500	100	200
160	2200	1500	1000	800	300	100	200
170	2300	1500	900	800	300	100	200
180	2500	1700	1200	800	400	100	200
170 °E	2400	2300	2000	1000	700	300	200
160	2500	3000	2200	1300	800	300	200
150	2500	4100	2800	1200	700	200	200
140	2500	4500	3500	900	600	200	200
130	2000	4400	5000	1000	800	300	200
120	1500	4400	4600	2300	700	400	200
110	1600	4000	x	2400	900	500	200
100	x	x	x	2000	1300	500	200
90	x	x	x	2300	1400	500	200

Table 5. Values of $\overline{k'\rho w'}$ (ergs cm^{-2} sec^{-1}) determined from Chart 4 for each grid point.

	20°	30°	40°	50°	60°	70°	80°
80°E	x	x	−30	−40	50	−30	−10
70	x	x	x	−10	40	−30	−10
60	x	x	−10	+40	00	−30	−10
50	x	0	−10	+30	−10	−30	−10
40	10	40	−10	+10	−10	−30	−10
30	−20	40	0	00	50	−30	−10
20	−30	40	40	−10	60	−30	−10
10	x	40	30	−20	50	−30	−10
0	x	0	40	−20	30	−30	−10
10°W	x	−20	−20	00	20	−20	−10
20	−20	−30	−40	10	00	−20	−10
30	−10	−30	−40	30	−10	−20	−10
40	0	20	100	30	−10	−20	−10
50	+50	150	200	00	−10	−20	−10
60	−50	−100	0	00	00	−20	−10
70	−240	−50	−30	50	100	−20	−10
80	0	200	0	00	50	−20	−10
90	0	−100	0	−30	00	−20	−10
100	200	400	−30	−10	00	−10	−10
110	150	120	0	−50	00	−10	−10
120	50	100	20	−100	00	−10	−10
130	−50	0	0	−50	−10	−10	−10
140	−30	−80	−50	−20	00	−10	−10
150	100	50	20	20	20	−10	−10
160	50	150	100	30	20	−10	−10
170	−100	60	80	30	20	−10	−10
180	−50	−30	20	00	10	−10	−10
170°E	50	−30	−20	−20	30	−10	−10
160	30	−80	−20	40	20	−10	−10
150	20	−180	−100	00	−10	−10	−10
140	0	−240	−150	−20	00	−10	−10
130	60	−100	−150	200	100	−10	−10
120	50	−100	−120	200	50	−10	−10
110	0	−100	x	50	50	−10	−10
100	x	x	x	−20	60	−10	−10
90	x	x	x	−30	60	−10	−10

Table 6. Values of $\overline{\phi' \rho w'}$ (ergs cm^{-2} sec^{-1}) determined from Chart 5 for each grid point.

	20°	30°	40°	50°	60°	70°	80°
80°E	100	200	400	450	150	280	−110
70	−70	0	100	100	0	360	−80
60	−230	−120	10	200	−260	420	−65
50	−180	30	110	200	−260	430	−50
40	0	170	200	−40	−300	430	−50
30	80	160	250	100	−250	420	−50
20	−120	−80	250	210	−130	330	−50
10	−220	−220	50	350	−50	200	−50
0	−220	−170	−120	210	−80	100	−60
10°W	−150	30	100	20	−160	50	−80
20	−50	200	170	−170	−220	40	−110
30	100	300	160	−320	−200	50	−140
40	200	360	190	−330	−40	50	−170
50	200	350	220	−170	180	50	−180
60	30	210	100	100	300	50	−190
70	0	330	20	250	260	80	−130
80	−100	400	−250	35	130	120	140
90	−180	−150	−100	−20	80	160	150
100	50	300	0	0	50	150	150
110	150	−100	−400	−50	−20	110	130
120	80	100	30	−300	−110	100	120
130	−140	0	0	−230	−200	100	90
140	−380	−250	−220	−410	−140	50	50
150	−440	−480	−300	−100	0	40	0
160	−150	−300	−80	420	100	20	−25
170	700	−110	260	1100	430	−30	−65
180	480	80	300	600	240	−80	−100
170°E	−230	240	−100	210	−50	−130	−125
160	30	210	280	210	−20	−190	−150
150	−20	−170	−80	90	−90	−230	−200
140	−300	−900	−600	−100	−200	−260	−215
130	−120	−300	−870	−700	−350	−270	−225
120	50	360	−300	200	−100	−250	−220
110	120	350	160	700	+150	−210	−210
100	215	380	400	600	+30	−70	−200
90	210	400	550	500	−20	+110	−150

Table 7. Tabulation of Correlation Coefficients (r) .

WMO No.	$r(k,\rho w)$	$r(\phi,\rho w)$	WMO No.	$r(k,\rho w)$	$r(\phi,\rho w)$	WMO No.	$r(k,\rho w)$	$r(\phi,\rho w)$
04202	−0.21	−0.40	72518	−0.24	−0.02	91245	0.08	−0.24
04270	−0.64	0.10	72572	0.05	−0.33	91250	0.13	−0.05
07170	−0.09	0.16	72637	0.41	0.41	91275	−0.21	0.40
07354	−0.03	−0.03	72645	−0.03	−0.38	91285	0.36	−0.39
08159	0.22	−0.08	72662	−0.05	−0.42	91334	−0.23	−0.08
08509	−0.13	0.22	72712	−0.19	0.07	91336	−0.19	−0.41
10610	−0.13	0.20	72734	−0.26	−0.09	98327	0.22	
47187	−0.44	0.25	72747	−0.18	−0.14	05238	0.16	−0.31
47931	0.09	−0.17	72768	−0.37	0.00	03548	0.68	0.27
60119	−0.06	0.16	72785	−0.58	−0.37	13040	−0.18	−0.12
62011	0.09	−0.15	72798	−0.28	−0.08	23464	0.08	0.21
70026	−0.12	0.03	72815	−0.09	−0.01	22522	−0.84	0.17
70200	0.05	0.06	72816	0.47	0.29	24688	−0.04	−0.13
70261	0.00	0.07	72836	0.07	0.09	26850	0.44	−0.13
70350	0.28	0.00	72879	−0.46	−0.22	27196	−0.09	−0.14
70398	0.00	−0.56	72913	−0.05	0.15	27612	0.24	−0.15
70409	−0.31	−0.24	72917	0.00	0.03	28698	0.51	−0.17
70454	0.06	0.06	72924	0.36	0.23	29514	0.36	0.01
72201	−0.17	0.06	72934	−0.16	−0.01	30758	0.22	0.32
72208	0.02	0.26	74082	−0.28	−0.50	31510	0.75	−0.20
72221	−0.18	−0.04	74795	0.14	0.10	31735	−0.13	−0.11
72235	0.00	−0.10	78016	−0.29	0.03	31960	−0.09	−0.27
72259	0.43	0.18	78063	0.05	0.29	32540	0.17	0.08
72261	0.25	0.13	78118	−0.36	0.15	33837	−0.06	0.19
72270	0.22	−0.07	78367	−0.34	−0.56	34560	0.10	0.00
72308	0.41	0.05	78806	0.02	0.10	35229	0.29	0.19
72405	−0.06	−0.28	78862	−0.16	−0.23	36177	−0.13	0.34
72456	−0.05	0.07	91066	−0.11	−0.01	38880	−0.30	−0.03
72469	−0.15	0.05	91115	−0.20	0.43	40597	0.00	
72493	0.26	0.09	91212	−0.03	−0.20	48900	0.00	
						62721	0.00	

Table 8. Values determined for $[\bar{K}'\rho\bar{w}']$ and $[\bar{\phi}'\rho\bar{w}']$ in ergs cm^{-2} sec^{-1} for each latitude circle.

Latitude	$[\bar{K}'\rho\bar{w}']$	$[\bar{\phi}'\rho\bar{w}']$
20	2.6	65.8
30	13.0	00.0
40	9.7	16.4
50	5.2	101.0
60	0.8	7.0
70	0.4	4.7
80	0.0	0.0

Table 9. Values determined for $\{[\bar{K}'\rho\bar{w}']\}$ and $\{[\bar{\phi}'\rho\bar{w}']\}$ in ergs cm^{-2} sec^{-1}.

$$\{[\bar{K}'\rho\bar{w}']\} = 7.5$$

$$\{[\bar{\phi}'\rho\bar{w}']\} = 46.0$$

Table 10. Values determined for $[\overline{k'\rho w'}]$ and $[\overline{\phi'\rho w'}]$ in ergs cm^{-2} sec^{-1} for each latitude circle.

Latitude	$[\overline{k'\rho w'}]$	$[\overline{\phi'\rho w'}]$
20	7.7	-13.2
30	3.9	43.7
40	-4.1	18.8
50	5.7	69.6
60	11.4	-15.9
70	-5.9	24.3
80	-1.7	-12.6

Table 11. Values determined for $\{[\overline{k'\rho w'}]\}$ and $\{[\overline{\phi'\rho w'}]\}$ in ergs cm $^{-2}$ sec $^{-1}$

$$\{[\overline{k'\rho w'}]\} \doteq 4.02$$

$$\{[\overline{\phi'\rho w'}]\} = 26.6$$

Table 12. Values determined for $[\overline{w'T'}]$ ergs gm $^{-1}$ sec $^{-1}$ for each latitude circle

Latitude	$[\overline{w'T'}]_{150-100\,mb}$	$[\overline{w'T'}]_{100-50\,mb}$
20	−.1	−.01
30	−.2	−.07
40	−.17	−.02
50	−.02	−.02
60	+.015	−.02
70	−.045	+.001
80	−.04	+.003

Table 13. Values determined for $\{[\overline{w'\alpha'}]\}$ for 150 to 100 mb and 100 to 50 mb.

	ergs gm $^{-1}$ sec $^{-1}$	ergs cm $^{-2}$ sec $^{-1}$
$\{[\overline{w'\alpha'}]\}$	.58	29.7
$\{[\overline{w'\alpha'}]\}$	.128	6.5

IV. DISCUSSION OF RESULTS

In this thesis the authors' aims were to attempt to determine the contributions of kinetic energy to the stratosphere by the advection term $\iint k\rho w\, dx\, dy$ and by the $\iint \Phi\rho w\, dx\, dy$ component of the source term. In addition, a value of the time eddy term of the conversion component of the source term was made available for the 150- to 50-mb level.

Postulation as to the sign of the energy conversion process in the stratosphere was that this conversion was from kinetic energy to potential energy (4), and this was verified by Nolan and White (3). Thus the stratosphere requires a replenishing of the lost kinetic energy in order to keep from running down due to dissipative processes.

The evaluation of the mean eddy term and the time eddy term of the advection of kinetic energy showed a positive contribution of 11.5 ergs $cm^{-2} sec^{-1}$. It is granted that this value is not the measure of the total advection term, but is believed to be our best figure for this term, at least until an explicit method is available to obtain $\bar{w}$ so as to make evaluation of $\{[\bar{k}][\rho\bar{w}]\}$ possible. The same reasoning is applied to the $\{[\bar{\Phi}][\rho\bar{w}]\}$ term. It is noticed that the contribution of the $\Phi\rho w$ component of the source term has a larger value than the advection term.

The time eddy contribution of the $\omega\alpha$ term gave the conversion component of the source term a value of -36.2 ergs cm^{-2} sec^{-1}. This figure is not representative of the complete atmosphere above 150 mb and its value was obtained from data to only 50 mb. It is believed that the direction of the conversion remains the same above 50 mb as from 150 to 50 mb but it is anticipated that the magnitude would be smaller. In addition, we received data to compute only the time eddy term, and not the mean eddy contribution plus other terms in the $\{[\overline{\omega\alpha}]\}$ expansion. According to White and Nolan (3) these other terms do not predominate, and it is the time eddy term that contributes the major portion to the $\{[\overline{\omega\alpha}]\}$ term.

It would thus appear that the advection term and the component of the source term are the modes by which the kinetic energy of the stratosphere is maintained and a net positive balance is available to balance the dissipative process. No values of are available at present.

Because our evaluation for the advection term is of small magnitude, this might imply that the systematic relation between k and $\rho\omega$ is very low and that no firm statement can be made about this term always being positive. Perhaps there is a more systematic positive relation between ϕ and $\rho\omega$ associated with the higher magnitude for the $\iint \phi\rho\omega \, dx\,dy$ term.

Unfortunately it was impossible, without very much more work, to give significance tests for these results.

Work being done by Jensen (6) has shown for the 850- to 700-mb level values of the advection term A to be near +500 ergs $cm^{-2}sec^{-1}$ in midlatitudes.

APPENDICES

Appendix 1: List of Symbols

Subscript 1 refers to 100-mb level

Subscript 2 refers to 200-mb level

^{1} Superscript refers to observation 12-hours previous

$\overline{\quad\quad}$ refers to average overtime

$[\ ]$ refers to average over latitude circle (E - W)

$\{\ \}$ refers to average over longitude circle (N - S)

C = magnitude of horizontal wind

$C_n = C_1^2 + C_2^2 + C_1'^2 + C_2'^2$

k = horizontal kinetic energy per unit mass = $C_n/8$

w = vertical velocity in x,y,z,t system

ω = vertical motion in x,y,p,t system

$\vec{F}$ = vector frictional force per unit mass

D = rate of frictional dissipation of kinetic energy

$\vec{k}$ = unit vector in vertical

dm = element of mass

$\vec{C}$ = horizontal wind vector

f = Coriolis parameter

ϕ = geopotential

R = gas constant for dry air = 2.87×10^{6} ergs $\text{gm}^{-1}\text{sec}^{-1}$

ρ = density

g = acceleration of gravity, 980 cm sec^{-2} value used

∇ = two-dimensional del operator

Z = vertical coordinate

α = specific volume

$\frac{d}{dt}$ = differentiation following a particle

$\frac{\partial}{\partial t}$ = partial differentiation (logical change)

t = time

p = pressure; vertical coordinate

x,y = horizontal space coordinates

θ = latitude

T = absolute temperature

γ_D = adiabatic lapse rate, or .98°C/10^4 cm

γ = existing lapse rate from sounding

Appendix 2:

The finite difference equation used by the AWS Climatic Center at Asheville, N. C., to compute 12-hour vertical velocities was as follows

$$W = - \frac{\left[\dfrac{\left.\frac{T_2+T_1}{2}\right|_{t=0} - \left.\frac{T_2+T_1}{2}\right|_{t=-12}}{\Delta t}\right] - \left[\dfrac{\left.V_1 V_2 \frac{\Delta\alpha}{\Delta h}\right|_{t=0} + \left.V_1 V_2 \frac{\Delta\alpha}{\Delta h}\right|_{t=-12}}{2}\right]\left[\dfrac{\left.(T_2+t_1)\right|_{t=0} + \left.(T_2+T_1)\right|_{t=-12}}{4}\right]\dfrac{\pi f}{(980)(180)}}{\gamma_d + \left[\dfrac{\left.\frac{T_2-T_1}{\Delta h}\right|_{t=0} + \left.\frac{T_2-T_1}{\Delta h}\right|_{t=-12}}{2}\right]}$$

where:

* Subscript 1 refers to lower level (200 mb)

* Subscript 2 refers to higher levels (100 mb)

" $t = 0$ refers to time of observation

" $t = -12$ refers to observation 12 hours previous

T_1, T_2 = temperature in °K (°C + 273.2)

V_1, V_2 = winds in cm/sec

$\Delta\,\alpha$ = wind direction at level two minus wind direction at level one measuring wind direction positive clockwise from north in degrees

$\Delta\,h$ = thickness of isobaric layer in cm

$\Delta\,t$ = 43,200 sec (12 hours)

γ_d = adiabatic lapse rate, or .98°C/10^4 cm

f = Coriolis parameter = $2\omega \sin \phi = 14.5\ (10^{-5}) \sin \phi\ \text{sec}^{-1}$

ϕ = station latitude

980 = approximate gravity with dimensions in cm sec^{-2}

w = vertical velocity in cm sec^{-1}

* This notation differs from the authors' since these symbols were set by Asheville.

Appendix 3: Statistical Analysis Methods

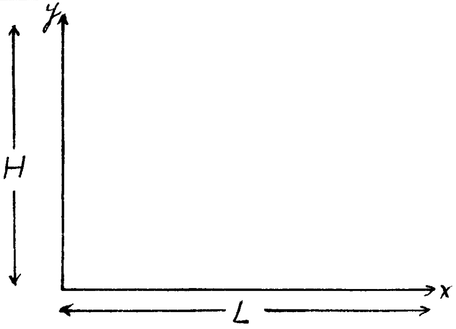

$k \equiv k(x,y,t)$

also $w = w(x,y,t)$

define

(1) $\bar{k} \equiv \frac{1}{T}\int_{0}^{T} k\,dt \quad ; \bar{k}(x,y)$

(2) $\bar{w} \equiv \frac{1}{T}\int_{0}^{T} w\,dt \quad ; \bar{w}(x,y)$

(3) $k' \equiv k - \bar{k} \quad ; k'(x,y,t)$

(4) $w' \equiv w - \bar{w} \quad ; w'(x,y,t)$

then

(5) $\overline{w'} \equiv \bar{w} - \bar{\bar{w}} = 0 \quad ; \overline{k'} = \bar{k} - \bar{\bar{k}} = 0$

(6) $kw \equiv (\bar{k} + k')(\bar{w} + w')$

(7) $\qquad \equiv \bar{k}\,\bar{w} + k'w' + \bar{k}\,w' + \bar{w}\,k'$

(8) $\overline{kw} \equiv \bar{k}\,\bar{w} + \overline{k'w'} + \bar{k}\,\cancelto{0}{\overline{w'}} + \bar{w}\,\cancelto{0}{\overline{k'}}$

(9) define: $[q] \equiv \frac{1}{L}\int_{0}^{L} q\,dx$ (q is a dummy variable)

(10) $q' \equiv q - [q]$

(11) $[q'] \equiv 0$

Now operate on $q = \bar{k}$ and $q = \bar{w}$

Then

(12) $\bar{k}\,\bar{w} \equiv (\bar{k}' + [\bar{k}])(\bar{w}' + [\bar{w}])$

(13) $\overline{kw} \equiv [\bar{k}][\bar{w}] + \bar{k}'\bar{w}' + [\bar{k}]\,\bar{w}' + [\bar{w}]\,\bar{k}'$

(14) $[\bar{k}\,\bar{w}] \equiv [\bar{k}][\bar{w}] + [\bar{k}'\bar{w}'] + [\bar{k}][\cancelto{0}{\bar{w}'}] + [\bar{w}][\cancelto{0}{\bar{k}'}]$

using equ (8)

(15) $[\overline{k\,w}] = [\bar{k}\,\bar{w}] + [\overline{k'w'}]$

substituting in from (14) for 1st term on rhs of previous equation

(16) $[\overline{k\,w}] = [\bar{k}][\bar{w}] + [\bar{k}'\bar{w}'] + [\overline{k'w'}]$

(17) Define $\{q\} \equiv \frac{1}{H}\int_0^H q\,dy$

(18) $q' \equiv q - \{q\}$

(19) $\{q'\} \equiv 0$

Now operate on $q = [\bar{k}]$; $q = [\bar{w}]$

(20) $[\bar{k}]\,[\bar{w}] \equiv \left(\{[\bar{k}]\} + [\bar{k}]'\right)\left(\{[\bar{w}]\} + [\bar{w}]'\right)$

(21) $\equiv \{[\bar{k}]\}\,\{[\bar{w}]\} + [\bar{k}]'[\bar{w}]' + \{[\bar{k}]\}\,[\bar{w}]' + \{[\bar{w}]\}\,[\bar{k}]'$

(23) $\{[\bar{k}][\bar{w}]\} \equiv \{[\bar{k}]\}\{[\bar{w}]\} + \{[\bar{k}]'[\bar{w}]'\} + \{[\bar{k}]\}\,\{\cancelto{0}{[\bar{w}]'}\}$
$+ \{[\bar{w}]\}\,\{\cancelto{0}{[\bar{k}]'}\}$

but from (16)

(24) $\{[\overline{k\,w}]\} = \{[\bar{k}][\bar{w}]\} + \{[\bar{k}'\bar{w}']\} + \{[\overline{k'w'}]\}$

We could substitute (23) for the first term on the right hand side of (24), but this we shall not do as these terms were not evaluated in our investigation.

The "time" eddy term, $\overline{k'\ \rho w'}$, was evaluated by the expansion

$$\overline{k'(\rho w)'} = \overline{k(\rho w)} - \bar{k}\overline{(\rho w)}$$

where ρ is just the density assumed constant at 150 mb. This term was computed for each station for the month, then plotted, analyzed and finally values were picked off at grid intersections (see data sheets) in order to complete the analysis and arrive at a single figure for the region between 20°N and 80°N.

The "mean" eddy term, $\bar{k}'\overline{\rho w}'$, was evaluated from the expansion

$$[\bar{k}'\overline{(\rho w)}'] = [\overline{k(\rho w)}] - [\bar{k}\overline{(\rho w)}]$$

where ρ is the same constant as above and where mean maps of k and ρw were utilized to effect the analysis of the "mean" eddy term (again see data sheets).

The terms representing the correlation coefficient in equation (23) may be further reduced as follows:

$$\overline{k'w'} = \overline{kw} - \bar{k}\,\bar{w}$$

$$\overline{k^2} = \frac{1}{64N}\Sigma\, C_n^{\,2}$$

$$\bar{k}^2 = \left[\frac{1}{8N}\Sigma\, C_n\right]^2$$

$$\overline{w^2} = \frac{1}{N}\ \Sigma\, w^2$$

$$\bar{w}^2 = \left[\frac{1}{N}\ \Sigma\, w\right]^2$$

For $r(\emptyset, \rho w)$, merely substitute $\emptyset$ in place of k in the above formulas.

Appendix 4: Data used for Maps

WMO No.	Number of Obs.	$\overline{w}$ cm sec^{-1}	$\overline{k'\rho w'}$	C_n $\text{cm}^2 \text{sec}^{-2}$	$\overline{Z}$	$\overline{\phi'\rho w'}$
04202	54	0.20	−11.8	415	13379	−221
04270	6	0.44	−11.7	387	13718	159
07170	54	−0.09	−11.1	792	13816	326
07354	56	−0.22	−74.2	1204	13867	61
08159	56	−0.12	35.7	1201	13943	−113
08509	54	−0.26	−40.2	2067	14104	214
10610	56	−0.003	−24.4	878	13813	338
47187	54	0.08	−218.4	3848	14197	668
47931	52	0.12	64.5	4672	14421	−255
60119	46	0.05	−16.2	2569	14098	160
62011	36	−0.10	61.9	6661	14154	−202
70026	28	0.02	−1.6	134	13586	26
70200	16	−0.08	.8	151	13656	33
70261	24	0.03	.00	110	13580	57
70350	40	−0.05	25.4	655	13725	1
70398	10	−0.08	−20.5	365	13795	−562
70409	36	−0.11	−18.3	691	13590	−460
70454	36	0.12	6.6	875	13672	1580
72201	38	−0.27	−134.3	3823	14427	64
72208	34	0.26	12.4	456	14212	577
72221	42	−0.16	−608.4	7595	14285	−189
72235	22	−0.30	4.4	4084	14235	−136
72259	40	0.19	426.1	6251	14170	359
72261	40	0.05	375.4	6795	14239	291
72270	38	0.10	117.8	4730	14205	−160
72308	36	0.09	301.6	4018	14060	123
72405	36	−0.16	−31.3	2950	14024	−623
72456	50	−0.06	−17.2	2660	14005	83
72469	52	−0.21	−76.9	2622	13985	−77
72493	36	−0.34	81.1	2433	14083	192
72518	52	−0.17	−75.1	2199	13931	−33
72572	42	−0.35	10.4	1797	13959	−474
72637	48	0.11	+105.0	2033	13946	52
72645	28	−0.21	−57.8	1146	13877	−554

WMO No.	Number of Obs	$\overline{w}$ cm sec^{-1}	$\overline{k'\rho w'}$	C_n cm^2 sec^{-2}	$\overline{Z}$	$\overline{\phi'\rho w'}$
72662	54	-0.11	-6.2	1524	13878	-388
72712	38	-0.12	-46.0	1612	13838	104
72734	44	-0.12	-53.0	1462	13868	-111
72747	50	-0.07	-28.1	1446	13821	-65
72768	26	0.12	-9.5	442	13799	0
72785	54	-0.05	-142.1	1562	13819	-377
72798	34	0.01	-31.9	954	13826	-115
72815	52	-0.10	-28.0	2099	13868	-24
72816	54	0.13	196.3	2084	13744	401
72836	16	-0.27	2.9	737	13831	35
72879	34	0.02	-15.0	408	13717	-97
72913	42	-0.02	-2.8	862	13645	766
72917	26	0.06	0.03	173	13411	14
72924	24	0.06	4.8	322	13462	107
72934	38	0.02	-4.2	495	13648	-19
74082	40	0.03	-5.1	249	13447	-142
74795	40	-0.20	278.8	6627	14311	240
78016	46	-0.31	-258.3	3582	14219	88
78063	34	-0.27	88.2	6097	14375	600
78118	58	-0.27	-237.2	2862	14457	208
78367	12	-0.20	-52.0	1769	14458	-162
78806	52	0.10	.8	248	14556	40
78862	58	-0.11	-35.0	1718	14511	-131
91066	10	-0.34	-10.8	1659	14289	-10
91115	50	-0.53	-230.9	4101	14450	-870
91212	44	0.12	5.7	329	14571	-79
91245	54	-0.06	54.7	2420	14535	-386
91250	46	0.08	12.9	410	14551	27
91275	40	-0.27	-186.6	2511	14493	880
91285	18	0.06	196.7	1957	14511	-360
91334	50	-0.09	-17.7	385	14583	-525
91336	18	-0.05	-9.0	277	14535	-265
98327	52	0.06	9.4	350		
05238	12	0.29	32.0	1560	14643	-583

WMO No.	Number of Obs	$\overline{w}$ cm sec^{-1}	$\overline{k'\rho w'}$	C_n $cm^2 sec^{-2}$	$\overline{Z}$	$\overline{\phi'\rho w'}$
03548	8	−0.24	232.5	2265	14253	422
13040	26	−0.33	−83.4	2674	14309	−252
23464	20	0.03	−30.7	2302	14292	358
22522	14	0.07	−95.3	934	13774	425
24688	36	−0.02	−2.4	450	13576	−235
26850	34	0.02	78.3	1054	13837	−225
27196	26	−0.10	−5.8	538	13786	−268
27612	46	0.13	11.9	502	13886	−812
28698	26	−0.29	46.8	1165	13794	−286
29574	36	0.13	57.9	1731	13672	13
30758	44	0.24	73.6	1940	13730	840
31510	22	−0.18	390.0	1068	13711	−776
31735	32	0.12	−19.8	972	13723	−274
31960	38	0.08	−89.0	5226	13953	−1680
32540	56	0.13	55.2	1258	13680	259
33837	18	0.15	−2.6	1055	13856	169
34560	20	0.06	5.7	1204	13920	3
35229	36	0.16	36.6	1025	13960	389
36177	18	0.16	−34.8	2282	13845	445
38880	6	−0.03	−8.9	1256	14157	−42
40597	11	1.045	0.1	2920	14655	−235
48900	21	.08	0.00	515	14655	24
62721	17	−1.58	0.4	2667	14485	70

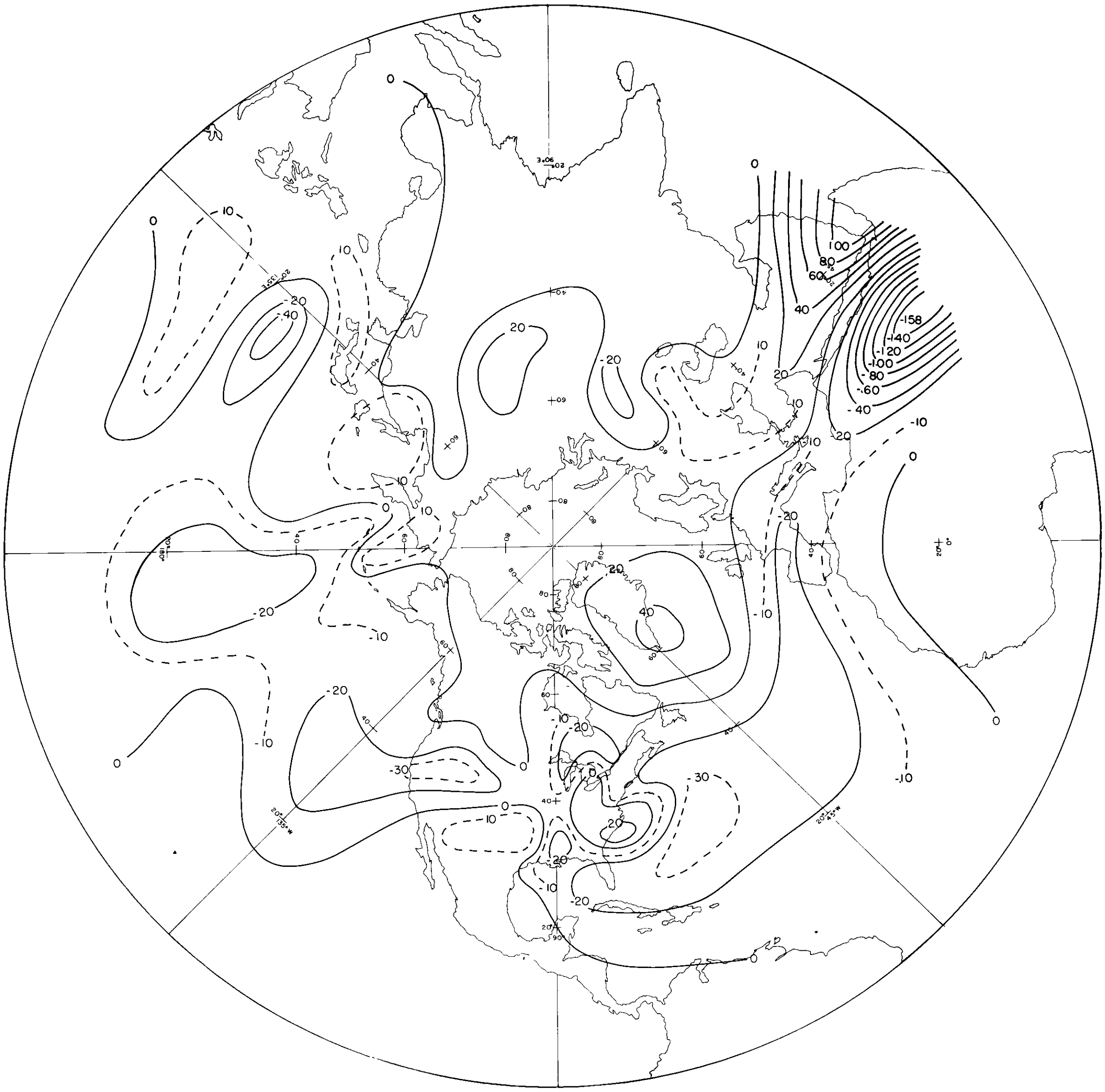

CHART 1. MEAN VERTICAL MOTION, $\tilde{w}$ (cm sec^{-1}), FOR THE 150-MB LEVEL FOR APRIL 1958.

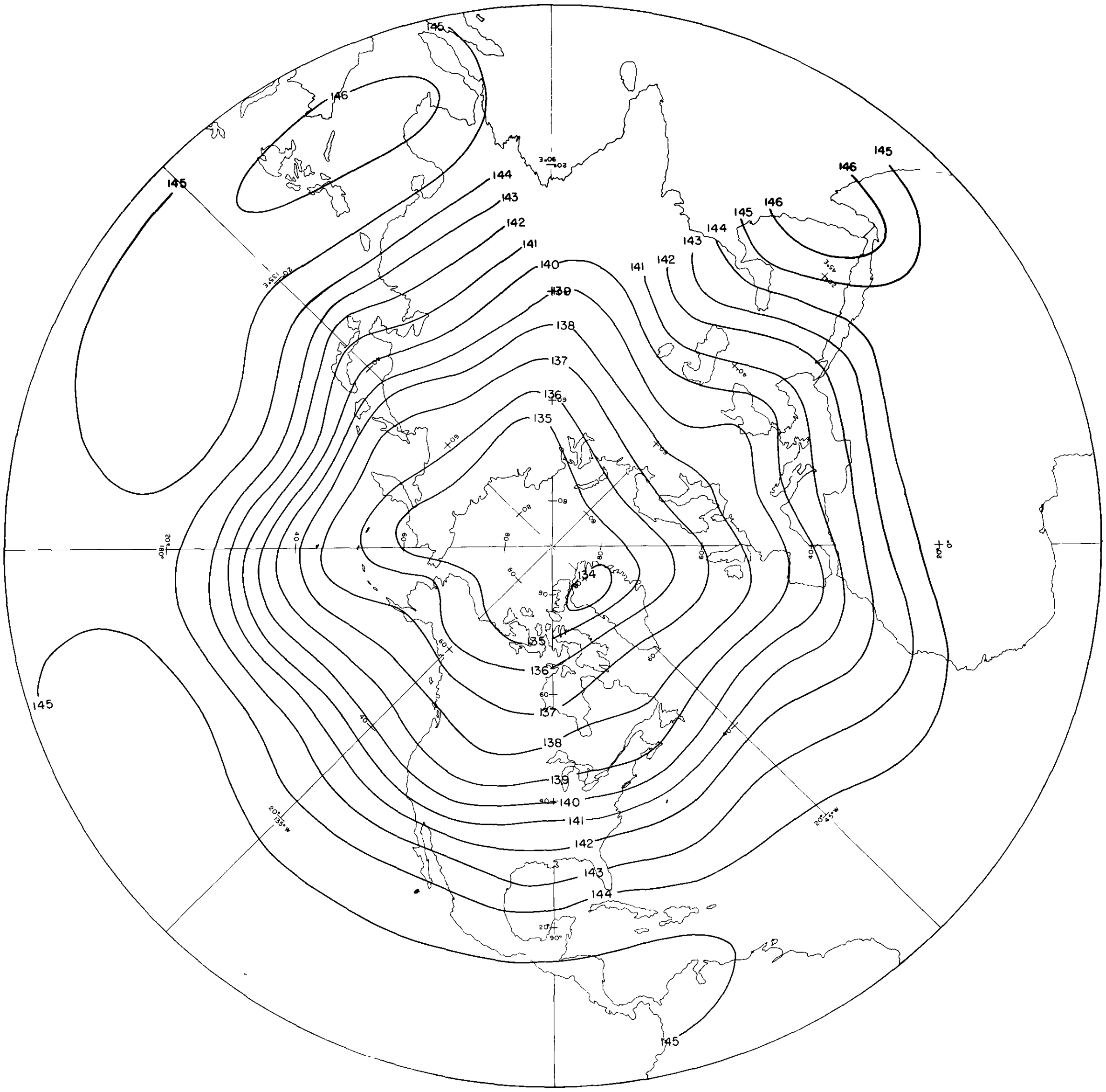

CHART 2. MEAN HEIGHT CHART, $\bar{Z}$ (meters), FOR THE 150-MB SURFACE FOR APRIL 1958.

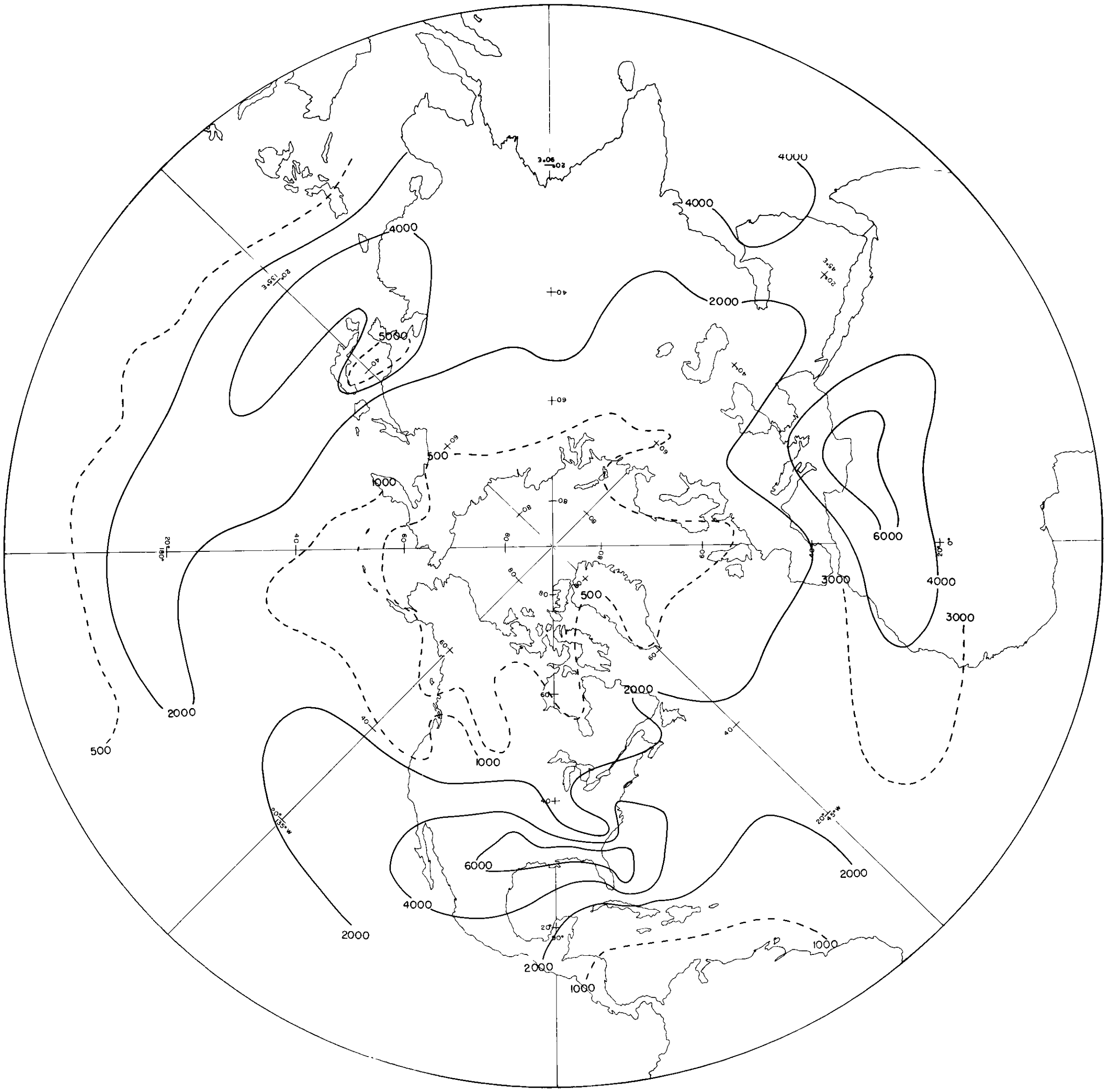

CHART 3. MEAN C_n (meters^2 sec^{-2}) CHART FOR THE 150-MB SURFACE FOR APRIL 1958 (TO DETERMINE $\bar{k}$ DIVIDE C_n BY 8).

CHART 4. MEAN TIME EDDY TERM, $\overline{k'\rho\ w'}$ (ergs cm^{-2} sec^{-1})FOR THE 150-MB LEVEL FOR APRIL 1958.

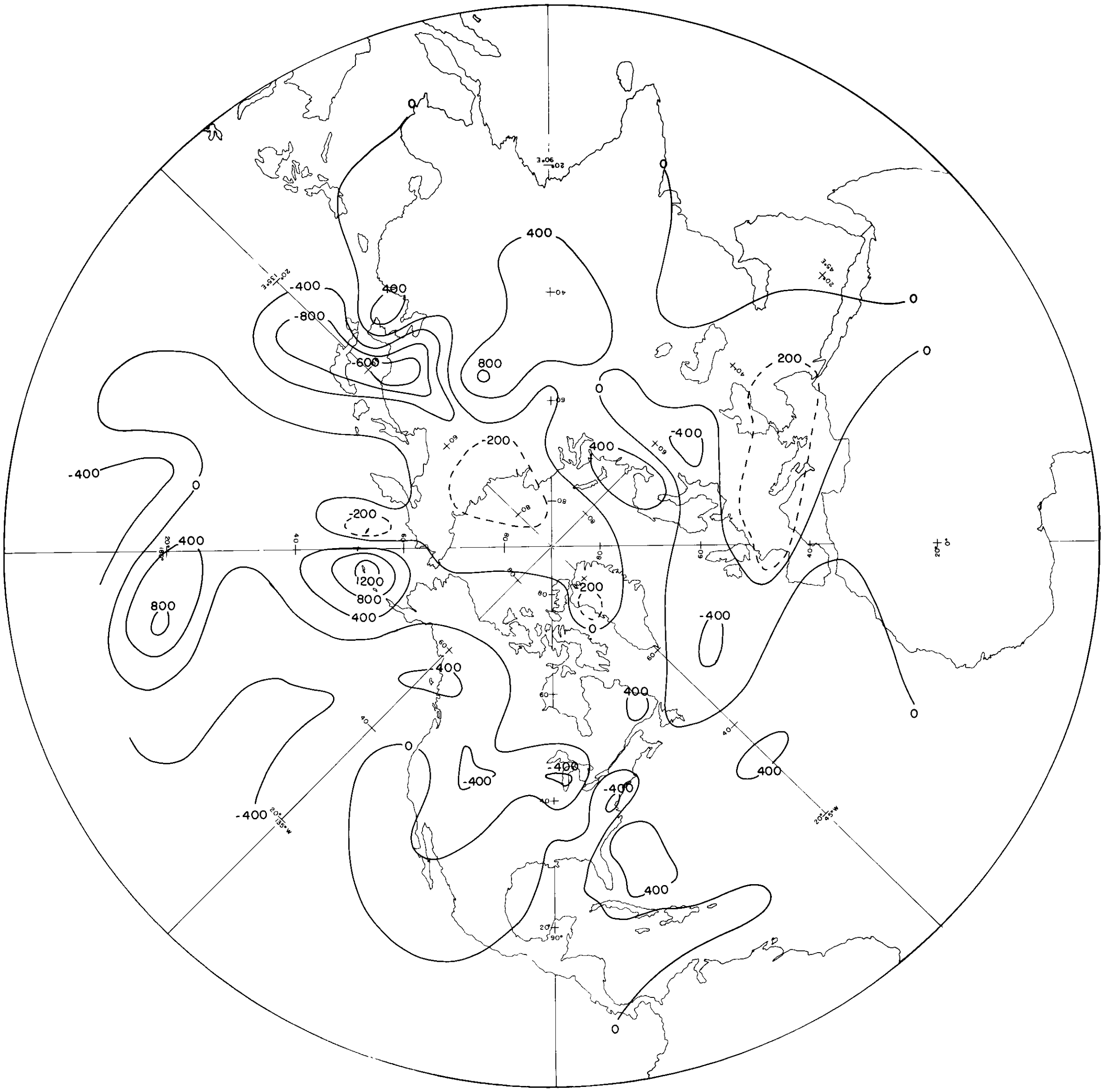

CHART 5. MEAN TIME EDDY TERM, $\overline{\phi'\rho\ w'}$ (ergs cm^{-2} sec^{-1}) FOR THE 150-MB LEVEL FOR APRIL 1958.

VI. REFERENCES

1. Saltzman, B., and A. Fleisher, 1959: The modes of release of available potential energy. Scientific Report No. 1, Planetary Circulation Project, Contract AF19(604)4958, MIT.
2. White, R. M., and B. Saltzman, 1956: On conversions between potential and kinetic energy in the atmosphere. Tellus 8, 357-363.
3. White, R. M., and G. F. Nolan, 1959: A preliminary study of the potential and kinetic energy conversion process in the atmosphere. To be published.
4. Starr, V. P., 1959: Questions concerning the energy of stratospheric motions. Scientific Report No. 1, Planetary Circulation Project, Contract AF 19(604)-5223, M.I.T.
5. White, R. M., 1954: The counter-gradient heat flux in the stratosphere. Tellus 6, 177-179.
6. Jensen, C. E., 1960: Doctoral Dissertation in Preparation. M.I.T.